

SUPPLEMENTARY INFORMATION

Climate change and Atlantic Multidecadal Oscillation as drivers of recent declines in coral growth rates in the Southwestern Caribbean

Luis D. Lizcano-Sandoval, Ángela Marulanda-Gómez, Mateo López-Victoria and Alberto Rodríguez-Ramírez

CT-Scanning

The CT-scanner used was the General Electric LightSpeed VCT 64-slice. The CT-scan provided several x-ray images from three different planes (Fig. S1). CT-scan images were saved in the DICOM format, with a resolution of 512 horizontal x 512 vertical pixels each, approximately. The images obtained by a CT-scanner and a x-ray differ in the how the degree of attenuation is measured. The attenuation of the images produced by a CT-scan is expressed in Hounsfield units (HU), instead of a gray scale as displayed by x-ray images. The degree of attenuation in CT-scan images indicates materials with different optical densities, and range from negative to positive HU values. For example, in a well-calibrated CT-scanner the optical density for air is <1000 HU, water is 0 HU, and dense bones are 1000 HU (Romans, 2011). These values allow to construct a calibration curve to estimate density of almost any material (i.e., aragonite).

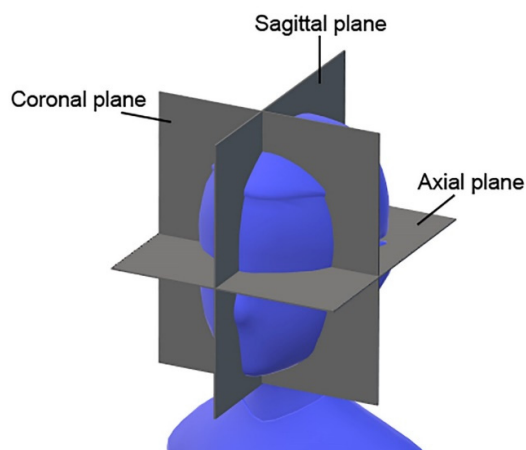


Figure S1. Imaging planes of a CT-scanner.

Coral cores were placed as shown in Fig. S2. An aragonite step-wedge standard was always placed in every scan. The settings used for coral cores of <1 m in length are shown in the Table S1. For future comparisons, we recommend to use similar thickness of coronal slices, pixel spacing and protocol parameters as here.



Figure S2. Placement/Positioning of coral cores for CT-scan. Polystyrene sheets were used to arrange and stack the coral cores.

DICOM images obtained were visualized in RadiAnt DICOM viewer v4.2. One image, from sagittal and coronal planes, was used for each core. The software ImageJ v1.51. was used to increase the image size from 512x512 to 2048x2048 pixels, which allowed to have more pixels per mm, and therefore increased the accuracy when estimating the linear extensions. As the direction in which the coral colony was growing may change along the coral core, appropriate transect paths were done following the main growth axis of the coral colony. Each transect provided values of distance in mm and optical density in HU. The DICOM images conserve the dimensions of objects, hence it was not needed to set a scale. The linear extension (cm yr^{-1}) and skeletal density (g cm^{-3}) were measured (see below for density calculations details), and the calcification rates ($\text{g cm}^{-2} \text{yr}^{-1}$) were calculated as the product of these parameters. Results from the coronal and sagittal images were averaged.

Table S1. CT-scan settings used for coral cores.

Scan options	Helical Mode
Slice thickness (mm)	5.625 (in coronal)
KVP	120
Protocol	Thorax/Abdomen
Exposure time (ms)	1825
X-Ray tube current (mA)	50
Exposure	2
Filter type	Body Filter
Convolution Kernel	Bone
Focal spot	0.7
Pixel spacing (mm)	1.918
Generator power	6000
Window center	53
Window width	2014

Calibration of density in $\text{gCaCO}_3 \text{ m}^{-3}$

A step-wedge standard obtained from giant clam shell *Tridacna gigas* with a known density of $2.86 \text{ gCaCO}_3 \text{ m}^{-3}$ was used to estimate coral density. We adapted a typical x-

ray method for coral growth analysis (Carricart-Ganivet and Barnes, 2007) to x-ray images produced by a CT-scanner. In theory, the CT-scan images should be similar to those produced by an x-ray machine. The different thickness of objects is visible and can be identified as an attenuation gradient (Thunthy and Weinberg, 1996; Fig S3).

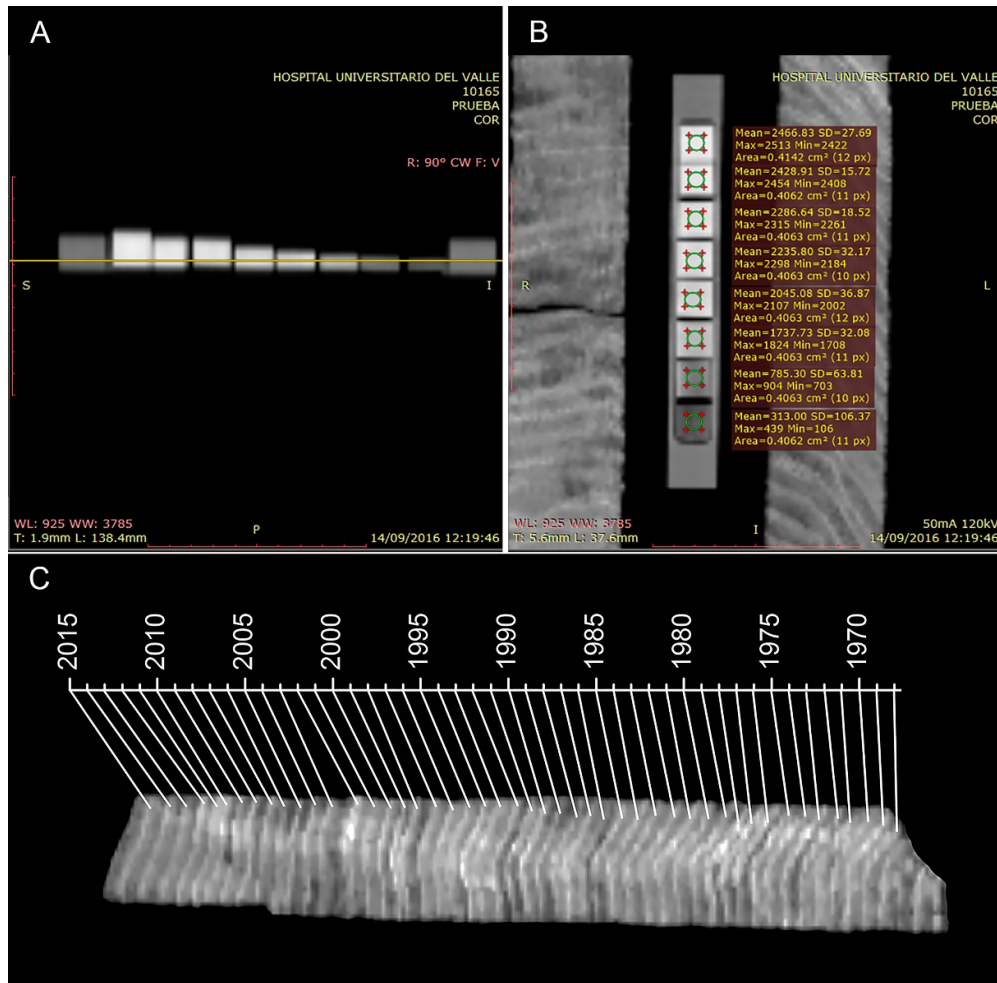


Figure S3. Example of CT-scan images of the aragonite wedge and a coral core. **(A).** A sagittal image of an 8-step-wedge standard from the giant clam shell *T. gigas* used to estimate coral density. The horizontal yellow line corresponds to the slice showed in the coronal plane (see next panel). **(B).** A coronal image of the aragonite wedge next to a coral core. Measurements of optical density (HU) were made on each step of the wedge from this plane. **(C).** An example of a dated coral core based on high and low density bands seen as lighter and darker bands, respectively.

A calibration curve (Fig. S4) was plotted using the optical densities (HU), the observed density ($2.86 \text{ gCaCO}_3 \text{ m}^{-3}$) and the thickness variation of the step-wedge. The skeletal density of the coral (g cm^{-3}) was estimated by fitting an exponential function to the optical density values obtained from a transect in the coral slice, and then divided by the slice thickness (cm).

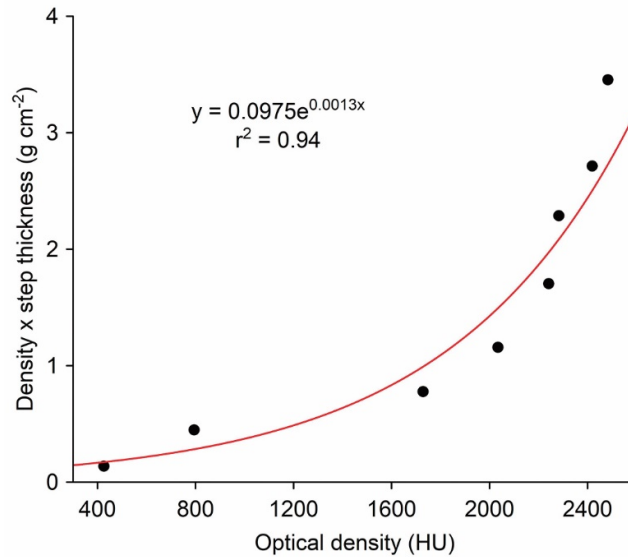


Figure S4. Exponential fit of the optical density (HU) vs. density x step thickness (g cm⁻²).

Advantages of CT-scan

Using the CT-scan method for coral growth analysis has several advantages: 1) There is no need to cut into slabs the coral cores as in the x-ray methods. 2) The CT-scan provides several x-ray images of coral cores in different planes, which allows to select the images where the density bands are better observed. 3) There are no radiation effects to be corrected as the heel effect (Duprey et al., 2012). 4) The density of the coral cores can be measured in HU, which are universal units for CT-scan machines, and a calibration curve to convert HU to gCaCO₃ m⁻³ can easily be made.

References

- Carricart-Ganivet, J. P., and Barnes, D. J. (2007). Densitometry from digitized images of X-radiographs: Methodology for measurement of coral skeletal density. *J. Exp. Mar. Bio. Ecol.* 344, 67–72. doi:10.1016/j.jembe.2006.12.018.
- Duprey, N., Boucher, H., and Jiménez, C. (2012). Digital correction of computed X-radiographs for coral densitometry. *J. Exp. Mar. Bio. Ecol.* 438, 84–92. doi:10.1016/j.jembe.2012.09.007.
- Romans, L. E. (2011). *Computed Tomography for Technologists: A Comprehensive Text*. China: Wolters Kluwer Health|Lippincott Williams & Wilkins.
- Thunthy, K. H., and Weinberg, R. (1996). Effects of tomographic motion, slice thickness, and object thickness on film density. *Oral Surgery, Oral Med. Oral Pathol. Oral Radiol. Endodontology* 81, 368–373. doi:10.1016/S1079-2104(96)80339-8.